5004-00-0004
Rev. 002

Post-Flight Report

HEMI Pathfinder Mission

Student Space Programs Laboratory
332 Electrical Engineering East, University Park, PA 16802
Phone: 814-867-2256

19 December 2008

This document does not contain proprietary information related to The Pennsylvania State University's Student Space Programs Laboratory (SSPL). This document is intended for public release.

Verify that this is the correct version before use.

SIGNATURES

Brian Schratz,
Project Manager, HEMI Pathfinder

Date

Kyle Holmes,
Project Scientist, HEMI Pathfinder

Date

Sven Bilén,
Director, SSPL

Date

(All Signatures on File with the SSPL)

REVISION HISTORY

Version	Date	Author	Description
001	9 Dec 2008	Brian Schratz	Initial Release

RELEVANT DOCUMENTS

Doc. Number	Title	Rev
n/a	HASP Call for Proposals	2007
n/a	HASP Student Payload Interface Manual	2008

*Relevant documents are available on the SSPL web server when available

ACRONYMS

CsI	Cesium Iodide
GRB	Gamma Ray Burst
HASP	High Altitude Student Platform
HEMI	High Energy Monitoring Instrument
JANUS	Joint Astrophysics Nascent Universe Satellite
MET	Mission Elapsed Time
NaI	Sodium Iodide
NASA	National Aeronautics and Space Administration
PMT	Photomultiplier Tube
PSU	The Pennsylvania State University
SP	Student Payload
SSPL	Student Space Programs Laboratory
UTC	Coordinated Universal Time

POST-FLIGHT REPORT

TABLE OF CONTENTS

LIST OF FIGURES

LIST OF TABLES

1.0 Overview

1.1 Introduction

This report describes the early development of the High Energy Monitoring Instrument (HEMI) for the detection of gamma ray burst peak energies to be included on the proposed future satellite mission, JANUS—the Joint Astrophysics Nascent Universe Satellite. This report is a review of the flight results of the first HEMI pathfinder, a cosmic ray detector, which was built over the course of nine months by students at The Pennsylvania State University's Student Space Programs Laboratory and launched successfully on a high altitude balloon on September 15, 2008.

1.2 Pathfinder Objectives

SSPL has developed a HEMI pathfinder experiment that flew on a short-duration, high-altitude balloon on 15 September 2008 from Ft. Sumner, NM. As GRB events are typically observed only once or twice per day, this balloon's 20-hour flight duration would not guarantee the observation of a GRB. Therefore, the scientific investigation focused on more common, low-charge cosmic rays. The development of this pathfinder cosmic ray detector balloon instrument gave students valuable experience that will be critical as they develop the GRB detection instrument for JANUS.

The pathfinder instrument's scientific objective was to distinguish cosmic ray particles by their charge (z = 1, 2, 3) and possibly an occasional cosmic shower. During a cosmic shower, the energies would be comparable to the normal background but the detection rates would be higher. Note that from this point forward, z represents the particle charge.

1.3 Detector

The baseline design for HEMI on JANUS is a traditional photomultiplier tube (PMT) with a scintillating crystal, likely NaI or CsI. To maintain as much heritage as possible between the HEMI pathfinder and the eventual HEMI for JANUS, the pathfinder used similar technology. Because of the different science objectives (cosmic rays for the pathfinder compared to GRBs for JANUS), short development time, less stringent requirements, and limited budget, the pathfinder detector was not exactly the same as the final one to be used on JANUS. The performance of the pathfinder PMT has a slower response (a few microseconds compared to a few nanoseconds), but the general characteristics of the PMT output pulse will be analogous to the eventual JANUS PMT.

2.0 Results

2.1 Flight Results

Launch occurred at NASA's Balloon Base in Fort Sumner, NM at 07:33:34 local time (MST) on 15 September 2008 (13:33:44 UTC). Table 1 shows the mission event timeline for key events during the flight in hours since launch, and both local and UTC time. The ascent lasted approximately two hours. The payload remained at float altitude (120,080 feet, 36.6 km) for 31.8 hours.

Table 1 Mission Event Timeline

Event	MET (Hours)	MET (hh:mm:ss)	Local Time	UTC Time
Launch	0.00	00:00:00	7:33:34	13:33:34
Achive Float Altitude	2.05	02:03:04	9:36:38	15:36:38
Local Noon	4.44	04:26:26	12:00:00	18:00:00
Local Sunset*	11.49	11:29:26	19:03:00	1:03:00
Local Midnight	16.44	16:26:26	0:00:00	6:00:00
Local Sunrise*	23.12	23:07:26	6:41:00	12:41:00
Instrument Power-down for planned termination	23.42	23:25:26	6:59:00	12:59:00
Instrument Power-up after termination cancelled	26.33	26:19:44	9:53:18	15:53:18
Local Noon	28.44	28:26:26	12:00:00	18:00:00
power down for final termination	32.36	32:21:47	15:55:21	21:55:21
Flight Termination	33.83	33:49:49	17:23:23	23:23:33
Local Sunset*	35.47	35:28:26	19:02:00	1:02:00

*Source: http://www.almanac.com/

Figure 1 shows the HEMI instrument at float altitude. At 17:23:33 local time on 16 September (23:23:33 UTC), HASP operators cut down the payload and it descended by parachute. After landing, the payload was recovered and HEMI was returned to PSU for post-flight calibration.

Figure 1 HEMI at Float Altitude

The first termination attempt began the morning of the second day. In preparation, most payloads including HEMI were turned off at 12:59:00 UTC on 16 September. When no optimal landing sites were available, HASP was allowed to float longer. Subsequently, some payloads, including HEMI were turned back on at 15:53:18 UTC. The payloads were finally powered off the final time at around 21:55:21 UTC in preparation for termination. HEMI was turned on before and through launch and ascent. The instrument continuously down-linked science and telemetry data throughout this time period.

The predicted minimum temperature of approximately –70 °F (–57 °C) was to occur around 60,000 feet. Ambient temperatures at float averaged 5 °C to 10 °C during the day and –40 °C at night. Figure 2 shows the temperatures of the top of the payload plate for two student payloads. Student Payload 12, or SP12 is one of the large payloads—the Microwave Reception Experiment—which characterized the spectrum between 45-75 GHz.. Student Payload 8 was not flown, and the temperature is of the mounting plate mounted away from HASP on a boom similar to the HEMI pathfinder. Note that the position of the payloads can affect a 20–30 °C difference in ambient temperature. Recall that the HEMI instrument was a small payload on one of the outrigger booms.

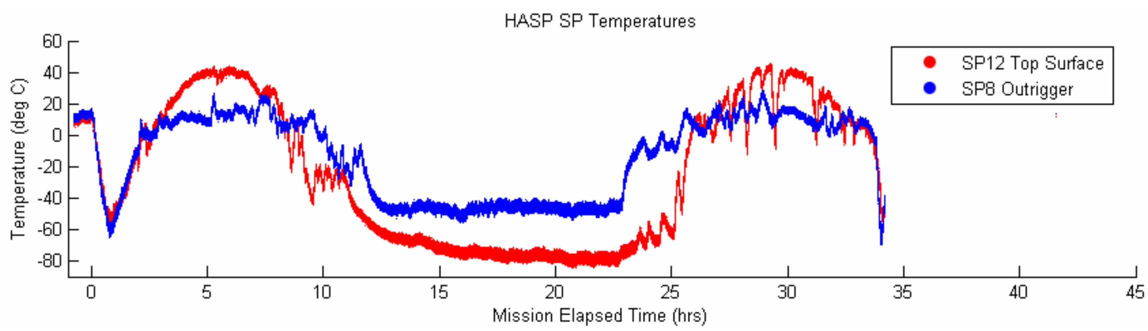

Figure 2 HASP Surface Temperatures

Figure 3 shows the data from the thermistor sensor placed on the PMT and monitored through the HASP analog channels. Comparing this to Figure 2 above shows that, despite previous (incorrect) calculations that the Earth's albedo and heat from the electronics would sufficiently warm the instrument, the internal temperature of HEMI in fact closely tracked the ambient environment temperature. Recall that the local sunset and sunrise times were at 11.5 and 23.1 elapsed hours, respectively. As the instrument electronics produced a constant amount of power, the only thermal variations were due to diurnal environmental variations. The only beneficial deviation from the ambient temperatures was that the PMT temperature only dropped to –30 °C as the balloon passed through the tropopause at roughly one hour into the flight, compared to the –60 °C ambient temperature. Of course this is still well below the +5 °C minimum operating limit of the PMT.

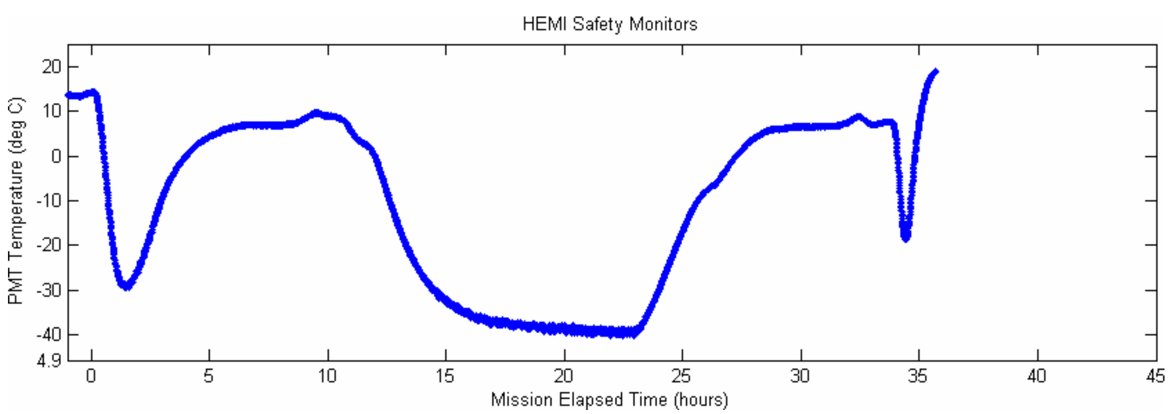

Figure 3 HEMI Safety Temperature Sensor

2.2 Science Results

The data product of the HEMI pathfinder was a recording of every peak voltage detected by the instrument throughout the mission. The data were stored on the ground in time-stamped data files, each containing 25,000 peak values. The majority of the peak values were noise around the threshold value, so the effective rate is 25,000 peaks about every 20 minutes or one time-stamped file every 20 minutes.

As soon as a new data file was available, a MATLAB script parsed the binary file and generated an energy spectrum showing the total number of counts (i.e., number of times a peak voltage occurred) during that time period versus the range of peak voltages.

Figure 4 shows three representative spectra taken during different times of the flight (indicated in the legends of each picture). The figures are marked with the local time (MST) as the local environment had an effect on the data, as will be described shortly. The tail end of the peak around 2 V is the noise present in the system. The C&DH peak detection algorithm included a software threshold to ignore peaks below 2 V. The large, distinct peak is due to muons. However, \the bottom two pictures deviate from the earlier calibration results in that multiple peaks and more distributed peaks are now visible.

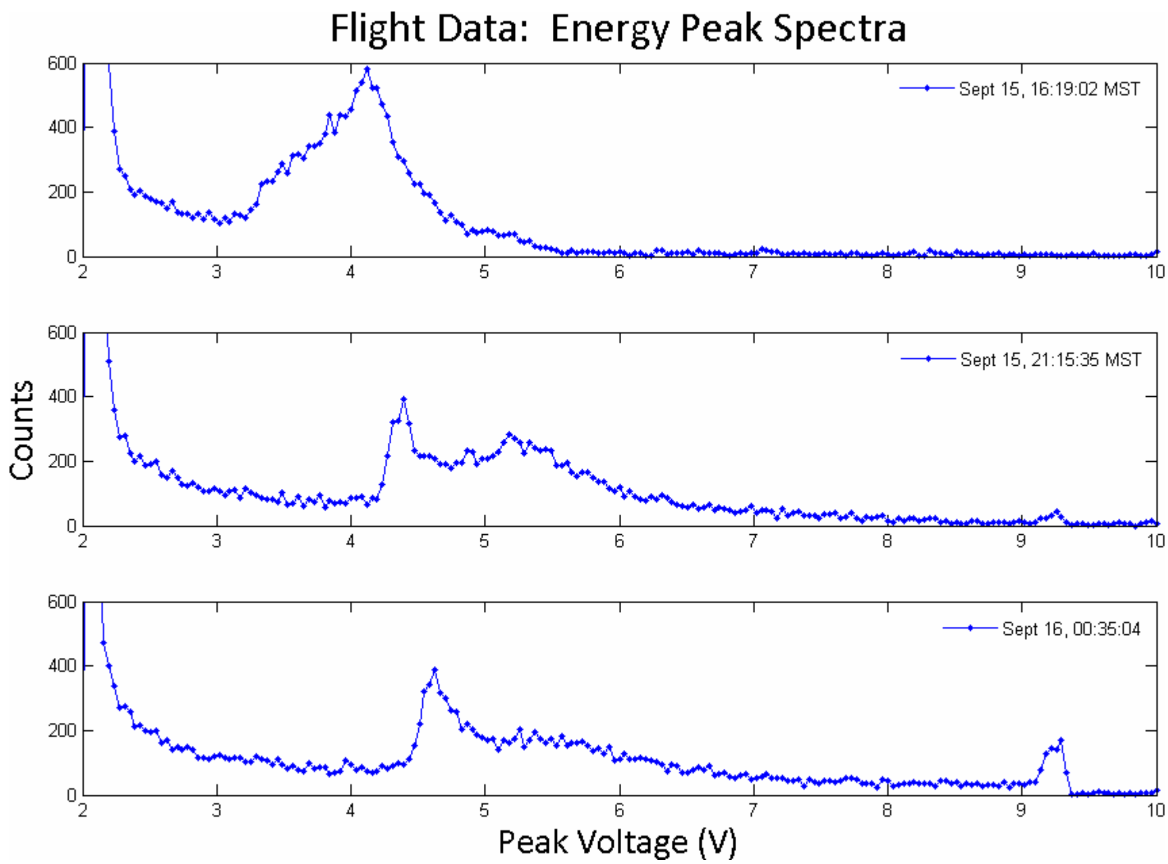

Figure 4 Select Energy Spectra Plots From Flight

Table 2 Spectra Time Stamps

Universal Coordinated Time (UTC)	Mission Elapsed Time (MET)	Local (MST)
Sept 15, 22:19:02	08:45:28	Sept 15, 16:19:02
Sept 16, 03:15:35	13:42:01	Sept 15, 21:15:35
Sept 16, 06:35:04	17:01:30	Sept 16, 00:35:04

Figure 5 shows how the energy spectra vary over the course of the flight. The *x*-axis is the mission elapsed time (MET) while the *y*-axis indicates the voltage of the peak(s) detected during each time interval. The color of the data point is indicative of how many times (counts) the peak voltage occurred during that time interval to indicate the relative size of each peak.

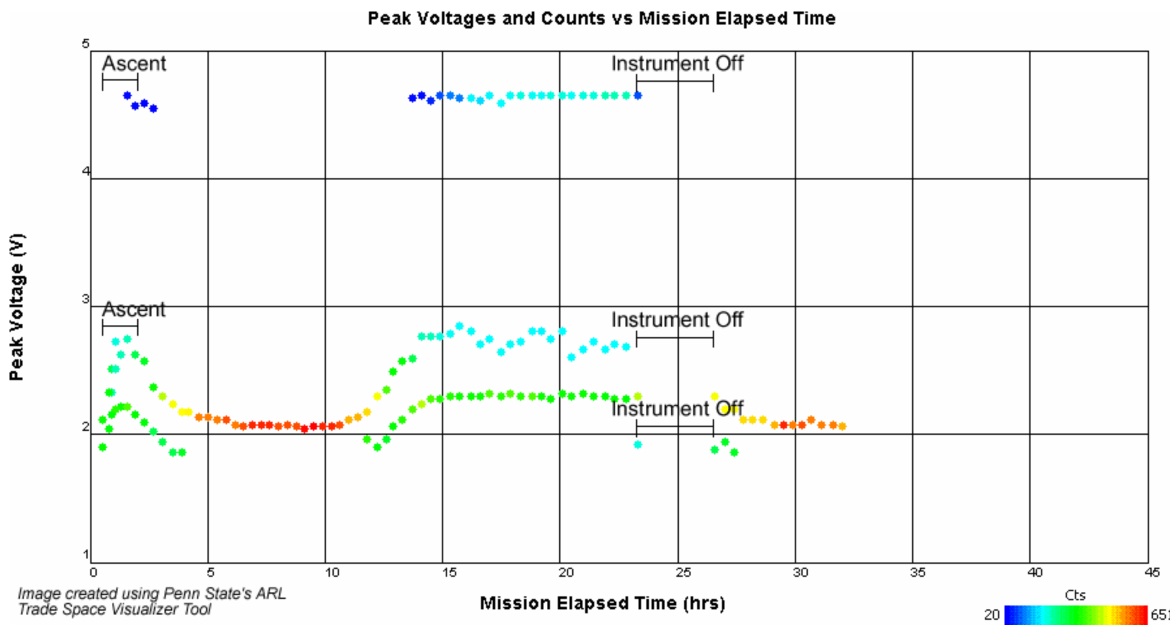

Figure 5 Peak Voltages and Counts vs. Mission Elapsed Time

By examining Figure 5, it is clear that there is a distinct diurnal variation in the data and that the rate and energy of the particle flux may vary with the Earth's rotation. However, the peaks did not agree with the expected z^2 energy relationship. Furthermore, the fact that the minimum temperatures far exceeded the operating and storage temperature of the PMT made the data suspect. Also, the NaI crystal is temperature sensitive, which could easily affect the data.

A post-flight calibration was carried out to verify that the temperature dependence hypothesis was correct. The full instrument was assembled and placed in the SSPL thermal-cycling chamber to simulate representative temperatures recorded during flight. Figure 6 shows the power consumption of the instrument and, most importantly, the temperature as it was measured by a thermistor mounted to the PMT.

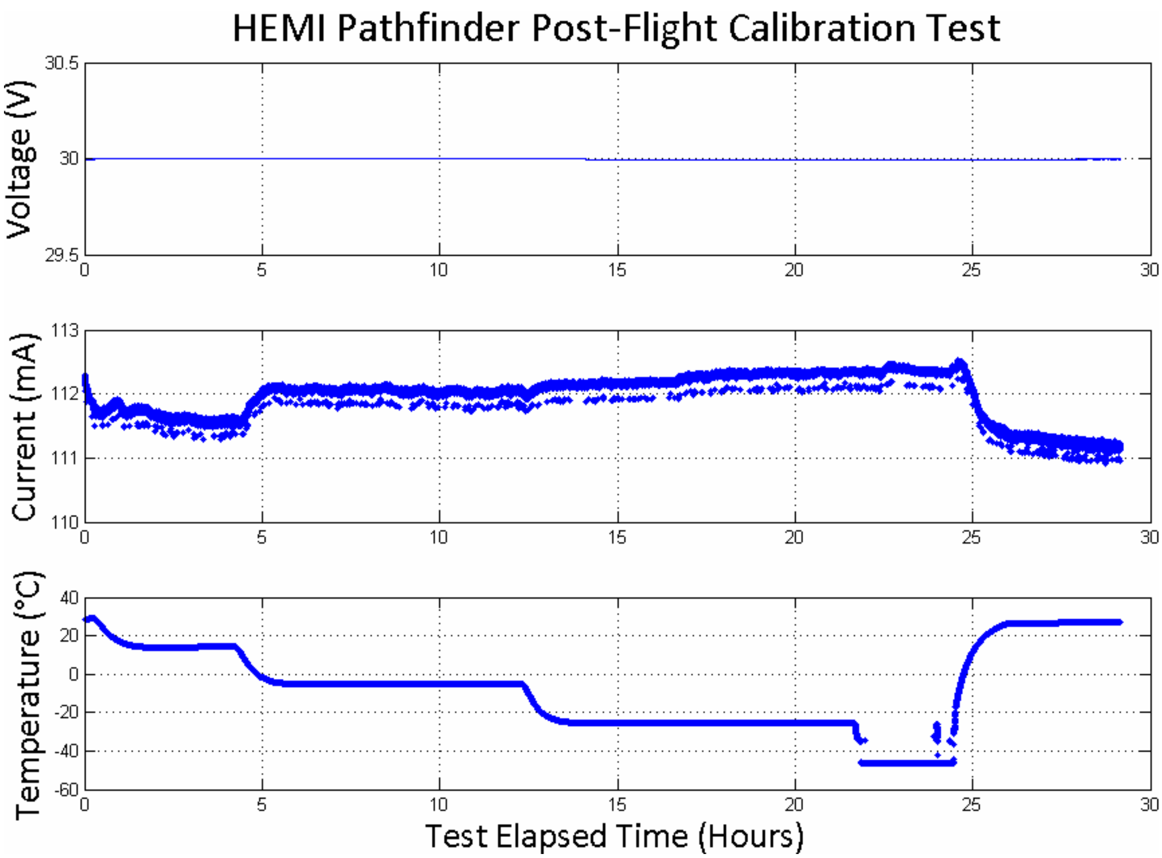

Figure 6 Post-Flight Calibration Environment

The instrument was left to operate at ambient room temperature for just under 12 hours. Afterwards the chamber was set to 14 °C, −5 °, and −30 °C as shown in Figure 6 above. The final drop between about 22 and 24 hours is explained by the AA batteries internal to the vessel powering the thermistor sensor getting too cold. The temperature chamber was maintained at −30 °C throughout this time. However, this was not noticed during flight.

The detector peak voltages during each of these periods are shown in Figure 7. One will quickly notice a drastic variation of peak values with the change in temperate. Also the constant ambient temperature periods before and after the test agreed nicely. This shows that the detector and electronics are not permanently damaged by exceeding temperature extremes but certainly vary with temperature. During temperature transitions, the distribution of peak voltages is significantly spread out as the temperatures vary. The soak periods, where the temperature is held constant, shows more distinct peaks. Finally, looking at the −30 °C soak, one will recognize the typical primary peak at 2.25 V and a more subtle secondary peak at 2.75 V. This agrees nicely with the values experienced during flight. The magnitude (number of counts) of the peaks is related to the time of each test period, with longer periods having more total counts. Therefore, the graphs below illustrate the relative trends of the peak as temperature changes.

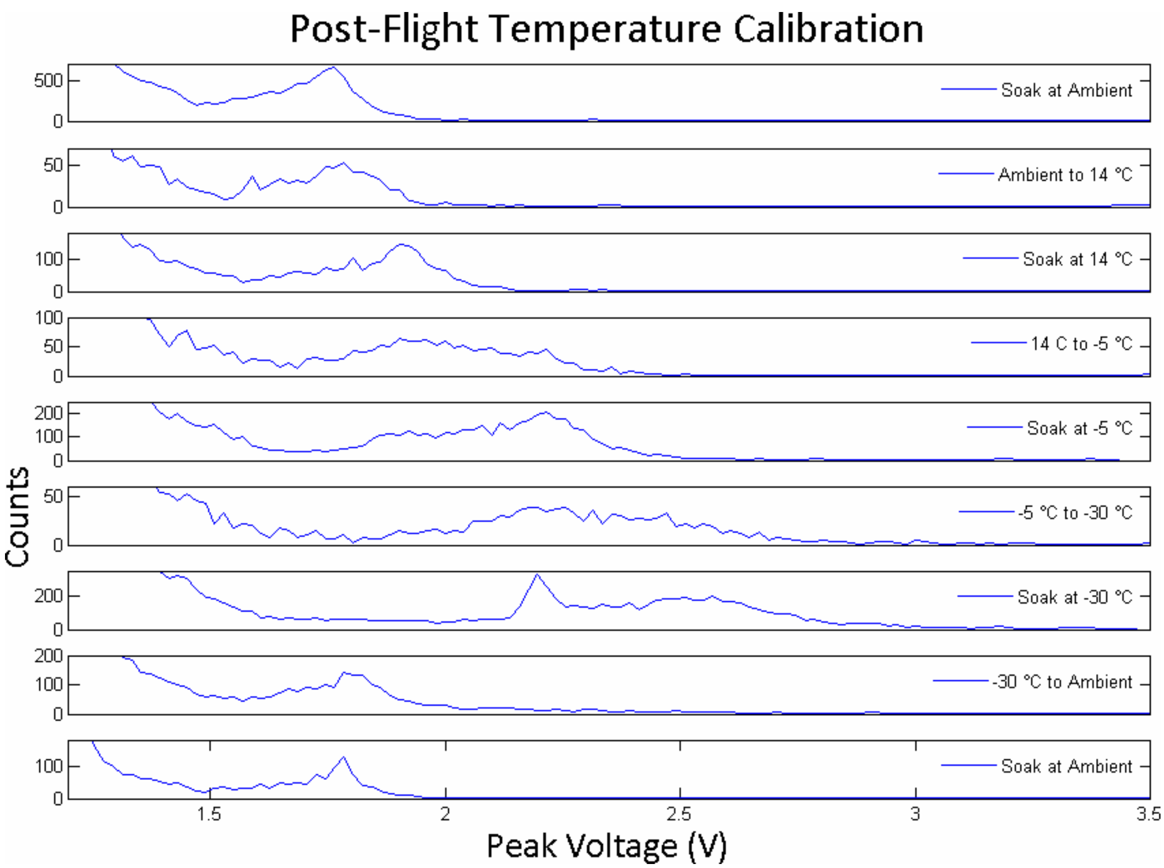

Figure 7 Varying Peak Voltages With Temperature

The only feature in the flight data that does not appear in the post-flight calibration data is the high energy peaks near the upper limit of the instrument output. If the muon peak voltage is centered at 2.25 V (at the extreme cold temperatures), then by the z^2 relationship, the expected peak for a $z = 2$ particle would be around 9 V. It is very likely that the upper peaks measured during flight were from particles from $z > 1$, but that the detector output just saturated. The more energetic particles do not penetrate to the ground altitudes.

It is clear now that the sensitivity of the detector and the selected gain provided so much amplification that only particles with $z = 1$ could be resolved. Any higher energy particles were collected in the single peak towards the end of the detector's range. Without access to energetic test sources with $z > 1$ for ground testing, it is impossible to verify this assumption. However, it is valid to conclude that in the flight configuration, only particles with $z = 1$ could be detected. Finally, if the originally planned uplink commands were implemented, at least the detector gain could have been lowered in near real time during flight, which may have given the detector enough dynamic range to detect the higher energy particles.

3.0 Project Summary

3.1 Conclusions

This effort was to educate and train a team of inexperienced students through the approximately 10-month development of a pathfinder energy detection instrument that would provide the foundation for the more complex and rigorous iterations to follow—eventually culminating as a flight instrument on the proposed JANUS mission.

The analysis of the flight data showed that thermal environment for high altitude balloons was not well understood for this mission and, as a result, the temperature of the electronics exceeded their operating ranges and the data during those extremes is unreliable. Furthermore, the inability to calibrate the detector with energetic sources expected during flight (~GeV) hindered the team's ability to understand the sensitivity and range of the detector output. As a result, only the lower-energy (low-z) muons were detected, as higher energy particles were outside the range of the detector in the flight configuration.

Despite these setbacks, the detector reliably detected muons during the nominal operating periods, which occurred during the local daytime when temperatures were within the operating range of the electronics. Furthermore, while not understood pre-flight, the anomalies experienced during flight were sufficiently understood and explained through extensive post-flight testing in the thermal chamber. Also, future iterations will be focused on lower energy gamma rays, for which the project has already acquired test radiation sources.

Therefore, from the science and engineering standpoint, the mission's minimum success criterion to detect and measure energetic particles during the flight was met. Comprehensive success would have been realized except for the schedule-driven de-scope actions that took place in the months prior to launch. These de-scopes allowed the minimum science objectives to be accomplished, but to do so, sacrificed the demonstration of up-link commands; remote operation and control of the instrument parameters (PMT gain, threshold level); and extensive system monitoring (although minimum monitoring was accomplished through the safety pressure and temperature sensors). It should be noted that the original designs allowed for such de-scopes in a methodical manner, in expectation that the short development schedule may require a limited focus.

On the programmatic side, it is the conclusion of the author that this project was an overwhelming success. It demonstrated an effective training and recruitment model that was able to train a young group of students in a matter of months and provide a strong personnel foundation for the next HEMI iteration on the long duration balloon. Despite being on a very constrictive schedule throughout most of the project, and especially towards the end, the project was able to generate comprehensive documentation on the prototypes, flight designs, testing, and integration—totaling 85 archived documents subject to unique document numbers and version control managed through SSPL's document library system. This total number does not include documentation of the post-flight analysis tools and results, which will be forthcoming upon completion of this report.

A wealth of knowledge and experience was generated during this project. The low student attrition rate in the near future will ensure that these lessons will not be forgotten, and this effort will provide a foundation for the continuing HEMI efforts. The lessons learned and heritage developed during this brief effort already serve as the foundation for the continuing HEMI project—now totaling 28 students and continuing to grow.

3.2 Future Work

A complete understanding of the incorrect pre-flight assumptions has to be investigated and documented. This final analysis will provide insight into the errors to be avoided in future efforts, specifically the thermal environment. The technical implementation errors are better understood at this point. That is, that thermal design needs to be revisited and better command and control of the instrument should be enabled. In hindsight it is reassuring that the original designs planned for all of this and it is regrettable that the resources available to the project were not sufficient to realize the full design within the schedule of the project. Also, the HASP designs, environment, and flight data will serve as a realistic example to validate the thermal model currently in development for the planned long duration balloon.

The intricacies of science and detector operations still leave room for improvement. The ground-tested PMT coincidence implementations were not as effective as was originally hoped or expected. The post-flight analysis forced many of the original understandings of the detector to be revisited. Completely relating the flight data to the scientific processes the data observed still needs to be done.

References

Band *et al*., "BATSE Observations of Gamma-Ray Burst Spectra. I. Spectral Diversity," *The Astrophysical Journal*, vol. 413, pp. 281–292, August 1993.

BATSE, (2005). The Burst And Transient Source Experiment. Web site: http://heasarc.gsfc.nasa.gov/docs/cgro/batse/

Butler, N.R., *et al*. "A Complete Catalog of Swift Gamma-Ray Burst Spectra and Durations: Demise of a Physical Origin for Pre-Swift High-Energy Correlations.," *The Astrophysical Journal*, vol. 671, pp. 656–677, December 2007.

CoBabe-Ammann, E., & Klumpar, D. (2008). *Final Report of the NASA Program Definition Team for Student Collaborations*. NASA.

Cusumano, G. *et al*. "Swift Observations of GRB050904: the Most Distant Cosmic Explosion Ever Observed," *Astronomy and Astrophysics*, vol. 462, pp. 73–80, February 2007

Feroci, M., Frontera, F., *et al*. "In-Flight Performances of the BeppoSAX Gamma-Ray Burst Monitor" *Proceedings of SPIE,* vol. 3114, pp. 186, August 1997.

Fox, D. B. *et al*. "The Afterglow of GRB 050709 and the Nature of the Short-Hard Gamma Ray Bursts," *Nature*, vol. 437, pp. 845–850, 2005.

Frail, D. A. *et al*. "An Energetic Afterglow from a Distant Stellar Explosion," *The Astrophysical Journal Letters*, vol. 646, pp. L99–L201, August 2006.

Gehrels, Neil (1998). Swift*: A Panchromatic Gamma Ray Burst MIDEX Mission*. Greenbelt, MD: NASA GSFC.

Gou, L. J., Fox, D. B., and Mészáros, P. "Modeling GRB 050904: Autopsy of a Massive Stellar Explosion at z = 6.29." *The Astrophysical Journal*, 668 (2007): pp. 1083.

HASP-CFP, (2008). *HASP Call for Proposals*. Baton Rouge, LA: Department of Physics & Astronomy, Louisiana State University.

HASP-SPIM, (2008). *HASP Student Payload Interface Manual*. Baton Rouge, LA: Department of Physics & Astronomy, Louisiana State University.

Knoll, Glenn F. *Radiation Detection and Measurement*. New York: John Wiley & Sons, Inc., 2000.

Liang, E. & Zhang, B. "Calibration of gamma-ray burst luminosity indicators," *Monthly Notices of the Royal Astronomical Society: Letters*, vol. 369, pp. L37–L41 2006, MNRAS, 269, L37

Murata, (2008). WP06R Datasheet. Retrieved November 27, 2008, from Murata Power Solutions, Web site: http://www.murata-ps.com/data/power/ncl/tdc_wp06r.pdf

National Semiconductor, (1995). PC16550D Universal Asynchronous Receiver/Transmitter with FIFOs. Retrieved November 26, 2008, Web site: http://www.national.com/ds/PC/PC16550D.pdf

"Paschen Curve." Teledyne Reynolds, Inc. 8 Oct 2008 <http://www.teledynereynolds.com/product/2multipin/page17.asp>.

Roming, Peter, et al. *Joint Astrophysics Nascent Universe Satellite: Observing the Illumination of the Universe*. Proposal to NASA SMEX AO. 2008.

Saint Gobain, (2008). Efficiency Calculations for Selected Scintillators.

Schratz, B. (2006). *Design of a Sounding Rocket Plasma Frequency Probe*. University Park, PA: The Pennsylvania State University.

Schratz, B. (2007). *High Energy Monitoring Instrument (HEMI)*. Proposal to NASA High Altitude Student Platform, 2008 Flight Opportunity.